UV-SPR biosensor for biomolecular interaction studies

F. A. Geiss[a,b], S. Fossati[a], I. Khan[a], N. Gisbert Quilis[a], W. Knoll[a], J. Dostalek[a*]
[a]Biosensor Technologies, AIT-Austrian Institute of Technology, Muthgasse 11, 1190 Vienna, Austria, [b]University of Natural Resources and Life Sciences, Gregor-Mendel-Straße 33, 1180 Vienna, Austria

ABSTRACT

UV surface plasmon resonance (SPR) for direct *in situ* detection of protein binding events is reported. A crossed relief aluminum grating was employed for diffraction coupling to surface plasmons as an alternative to more commonly used attenuated total reflection method. Wavelength interrogation of SPR was carried out by using transmission measurements in order to probe odorant-binding protein 14 (OBP14) of the honey bee (*Apis mellifera*). The native oxide layer on the top of an aluminum grating sensor chip allows for covalent coupling of protein molecules by using regular silane-based linkers. The probing of bound OBP14 protein at UV with confined field of surface plasmons holds potential for further studies of interaction with recently developed artificial fluorescent odorants.

Keywords: plasmonics, diffraction grating, UV, aluminum, odorant binding protein

1. INTRODUCTION

Surface plasmon resonance (SPR) has become an established technology for biomolecular interaction analysis and for detection of chemical and biological species [1]. This method offers the advantage of direct detection principle and it finds its applications in important fields of medical diagnostics and food safety [2, 3]. The majority of SPR biosensors utilize sensor chips with gold films or gold nanoparticles in order to probe the captured target analyte with the confined surface plasmon field at wavelengths in the green, red or near infrared part of spectrum. The use of silver instead of gold offers the advantage of lower Ohmic losses and possible SPR probing at lower wavelengths in the blue part of the spectrum [4]. In recent years, aluminum becomes increasingly explored for SPR sensing at even lower wavelengths in UV part of spectrum [5, 6]. It is worth of noting that surface plasmon excitation at aluminum occurs at wavelength as low as 200 nm [7-9]. Besides SPR-based sensors, aluminum plasmonic structures were explored in other fields including surface plasmon-enhanced fluorescence [5, 10, 11], thin film solar cells [12], and chromatic nanostructures [13].

In contact with air, a native oxide layer is formed on the top of aluminum films, which provides similar chemical inertness as gold. The thickness of this layer is mostly reported as 2-3 nm [5, 14, 15], which is much smaller than the penetration depth of surface plasmons and does not prevent its utilization for sensing [10]. The oxide passivation layer enables functionalization by using silane linkers instead of thiols that are most often used for gold. The probing with surface plasmons at UV wavelengths in aqueous environment holds potential for increasing detection sensitivity of direct SPR biosensors and it offers means for the implementation of plasmon-enhanced fluorescence [10, 11, 16] for several analytes that exhibit inherent absorption in this wavelength range. These include DNA, proteins (absorption bands at 200 - 280 nm), various odorant binders [17, 18], and e.g. aflatoxins [19]. However, the probing of the aluminum sensor surface with light at UV wavelengths imposes several challenges. The increasing absorptivity of the high refractive index optical glasses in the UV requires usage of fused silica [20]. Therefore, the commonly used attenuated total internal reflection method with a prism made of such low refractive index glass does not allow reaching the high momentum of the incident light needed for the phase matching with surface plasmons. Thus, the resonant excitation of surface plasmons on aluminum surfaces allowed the probing only *ex situ* on dry sensor chips, while *in situ* measurements of kinetics of surface reactions in contact with water were not reported.

In order to overcome the above-mentioned restrictions, the using of aluminum grating-coupled SPR sensor is reported for the *in situ* observation of proteins at UV wavelength of 280 nm in an aqueous environment. According to the knowledge of the authors, wavelength interrogation of SPR is utilized for the first time for the observation of molecular

*jakub.dostalek@ait.ac.at; phone +43 50550 4470; fax +43 50550 4450; www.ait.ac.at

binding events in aqueous environment in this wavelength range, which is not possible for the more commonly used Kretschmann-Raether geometry. As model analyte, the odorant-binding protein 14 (OBP14) of the honeybee (*Apis mellifera*) [21] is used, which might be of interest for odorant binding analyses with recently developed artificial fluorescent odorant analogues that absorb in the UV-range [18].

2. MATERIALS AND METHODS

Chemicals

Microposit S1805 was obtained from Shipley, the developer AZ 303 from MicroChemicals. Polymethylsiloxane (PDMS) elastomer Sylgard 184 was acquired from Dow Corning and Amonil MMS 10 (Amonil) from AMO GmbH. Tris(hydroxymethyl)aminomethane hydrochlorid (TRIS-HCl), dimethylsulfoxid (DMSO), bis(carboxymethyl)-L-lysine, Hellmanex III solution, and $NiCl_2$ were purchased from Sigma-Aldrich. 11-Pentafluorophenylundecanoate-triethoxysilane was obtained from Sikemia. The odorant-binding protein 14 (OBP14) from *Apis mellifera* with histidine tags was kindly provided by the group of Prof. Paolo Pelosi of the Department of Biology of Agriculture, Food and Environment, University of Pisa, Italy.

Preparation of the aluminum crossed gratings

UV laser interference lithography (LIL) was used for the preparation of crossed grating structures utilizing Lloyd's mirror configuration and a HeCd laser that operated at a wavelength of 325 nm (IK 3031 R-C, purchased from Kimmon). A 400 nm thick layer of Microposit S1805 photoresist was deposited on a BK7 glass substrate by spin-coating (45 s, 4500 rpm), followed by soft baking for 120 s at 98 °C. These substrates were exposed to the interference field with the intensity of 32 µW/cm^2 at an angle of 54.34 deg, which corresponds to a grating period of Λ=200 nm. In order to record a crossed grating structure, the exposure was carried out twice for two orientations of the sample with a rotation angle of 90 deg. The exposed samples were developed with the developer AZ 303 that was diluted by distilled water at a ratio of 1:14.

Replicas of the relief LIL grating were prepared by UV nanoimprint lithography (NIL). The prepared photoresist crossed gratings were casted to PDMS, followed by a curing step for 3 days at room temperature. The PDMS copy was detached from the master and employed as a working stamp. These working stamps were used for the preparation of series of Amonil gratings on the top of UV-transparent fused silica glass substrates (from Neubert-Glas). The fused silica glass substrates were cleaned for 10 min in an ultrasonic bath with Hellmanex III solution (2 %) and successive rinsing by water and ethanol. Afterwards, Amonil MMS 10 was spin-coated at 2000 rpm for 120 s, which corresponds to a layer thickness of 110 nm ± 5 nm. Then, the PDMS stamp was placed on the top of the Amonil layer which was subsequently irradiated by UV light (UV lamp Bio-Link 365 from Vilber Lourmat with the wavelength λ = 365 nm). The irradiation dose was set to 5 J cm^{-2}. Finally, the PDMS stamp was detached from the cured Amonil MMS 10, leaving a copy of the master structure in the crosslinked polymer layer. The obtained crossed grating structures were coated with 20 nm of aluminum by vacuum thermal evaporation (HHV AUTO 306 from HHV Ltd.) in a vacuum of at least 10^{-7} bar. Samples without the corrugation were prepared in order to serve as reference.

Surface modification of aluminum gratings

For the attachment of the protein, the two commercially available linker molecules 11-Pentafluorophenylundecanoate-triethoxysilane and bis(carboxymethyl)-L-lysine were allowed to react overnight in water-free DMSO (stored over a molecular sieve) to form an appropriate linker for protein attachment onto aluminum, having a silane and a nitrile tri-acetic acid (NTA) groups at the opposite ends, see Figure 1 (10 mM each in 1 mL DMSO). The product was pipetted on the aluminum chip with native oxide on the top and incubated until the DMSO was completely evaporated (volume of 200 µL was spread over an area of 4 cm^2). This procedure was repeated twice. Subsequently, the linker was stored at 80 °C for two hours. Afterwards, the chip was rinsed with DMSO to remove the unbound linker molecules and then with pure water to remove the DMSO. The chip was incubated with 0.1 M $NiCl_2$ solution for 30 min to obtain Ni^{2+}-NTA

residues by the formation of complex bonds between the Ni^{2+} and the NTA residues. The chip was rinsed again with water and afterwards 200 µL of 10 µM OBP14 were applied in 5 mM TRIS-HCl buffer (pH=8) by pipetting droplets on the chip surface until the surface was completely covered with protein solution for incubation overnight, which took place in a Petri dish with a wet paper towel to avoid the drying of the chip surface by maintaining the air humid.

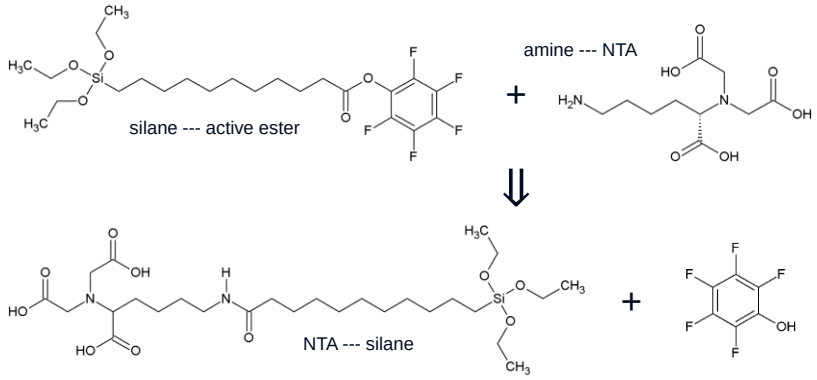

Figure 1. Reaction of the crosslinkers 11-Pentafluorophenylundecanoate-triethoxysilane and bis(carboxymethyl)-L-lysine to an NTA-silane product, capable to be tethered onto an alumina surface via the silane group and to bind a his-tagged protein via the NTA group (Ni^{2+} has to be added to form Ni^{2+}-NTA before protein attachment occurs). The linker reaction took place in water-free DMSO.

Optical setup for UV-SPR measurements

A custom-made optical system was employed to characterize the plasmonic properties of the prepared aluminum grating sensor chips. A schematic of this setup is presented in Figure 2. Light from a Xe lamp (LSB510 lamp with LSA122 adapter, LSH102 housing and LSN151 power supply from Lot Oriel) was collimated with a UV silica lens (LA4052-ML from Thorlabs), passed through a polarizer (WP12L-UB from Thorlabs) and the aluminum grating sensor chip. Against the sensor chip, a flow cell with a quartz glass substrate and a PDMS gasket (volume of 10 µL) was attached. The sensor chip was mounted on a rotation stage (DT 40-D25 from Owis) to control the angle of incidence θ. The transmitted light beam was focused with a fused silica lens at an optical fiber (M92L01 from Thorlabs) and analyzed with a spectrometer (Andor Shamrock SR-303i-B equipped with an Andor CCD detector DU920P-OE). The transmission spectra measured for the Al grating samples were normalized with that measured for identical layer structure on a flat substrate without the grating.

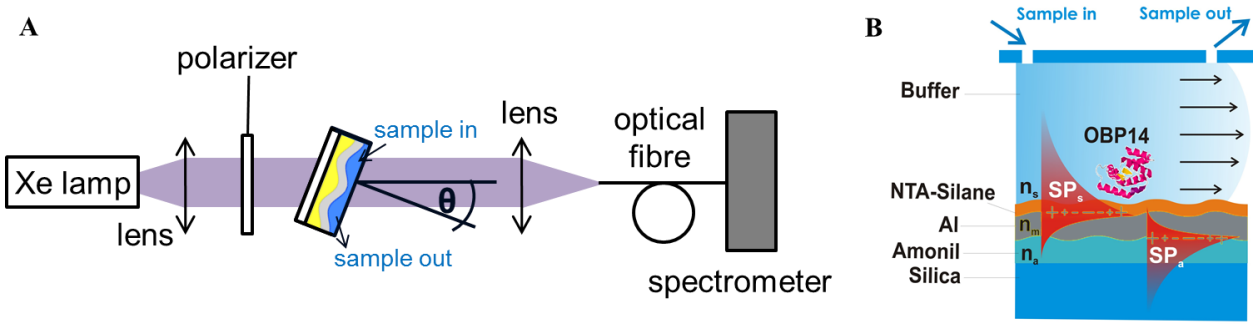

Figure 2. Schematics of the transmission setup which was used for UV-SPR measurements (A) and layer structure of the prepared aluminum grating sensor chip (B).

Simulations

Optical simulations on diffraction coupling to surface plasmons were carried out by using the integral method implemented in the software PCGrate, version 6.6. The used parameters were p-polarized incident light, a sinusoidal grating with Λ=200 nm and 30 nm modulation depth. The refractive index of aluminum n_m was taken from the handbook of Edward D. Palik [22], which is included in the software library. The refractive index n_s of water and air were obtained from Hale & Querry, 1973 [23], and Ciddor, 1996 [24], respectively. Refractive index of Amonil n_a=1.57 was taken from the data sheet of the AMO GmbH. The simulations were performed in a range from 200-500 nm and an increment of 1 nm. Each polar angle was simulated separately. Curves were simulated with regard to transmission efficiency of the zeroth order and absorption. Data were exported to Microsoft Excel and afterwards evaluated, e.g. 3D plotting, using Origin Lab 8.5.

3. RESULTS AND DISCUSSION

Morphology of prepared Al gratings

The sensor chips carrying an Al grating were at first observed in air with AFM (PicoPlus from Molecular Imaging, Agilent Technologies) in tapping mode. The acquired topology of the prepared structure is showed in Fig. 3. It reveals a crossed grating with a period of Λ=200 nm and a depth of around 30 nm. The area of the sensor chip was 2×2 cm^2.

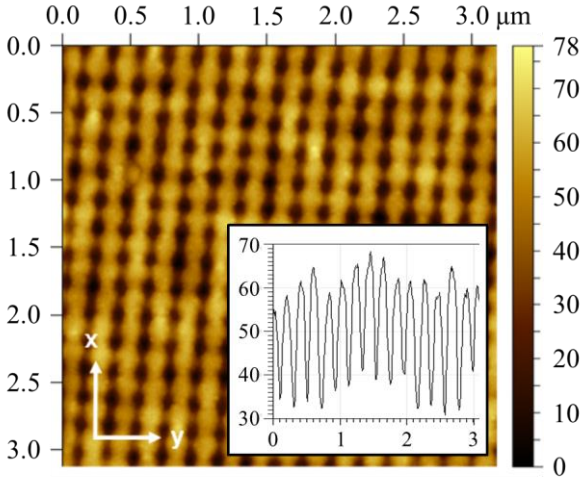

Figure 3. Characterization of a crossed Al grating by AFM. Profile cross-section is shown as inlay (scale is in µm).

Resonant excitation of surface plasmons on Al grating

Transmission wavelength spectra were measured for the aluminum grating that was brought in contact with air and with buffer (5 mM TRIS-HCl with pH=8) and the angle of incidence was varied in the range θ=0 - 30 deg. The acquired wavelength transmission spectra were normalized with those measured for a plane sensor chip without grating. The experimental results are compared with simulations in Figure 4. Firstly, dependence of absorption on the wavelength and angle of incidence θ was used in order to identify dispersion of excited surface plasmon modes at the air-aluminum and Amonil-aluminum interfaces. Figure 4A reveals the excitation of two of these surface modes at the interface with a sample (SP_s) and Amonil (SP_a) which is manifested as increased absorption. The resonant excitation of surface plasmons travelling along the air interface with a normally incident beam θ=0 deg occurs at the wavelength of λ=214 nm. For the interface with Amonil, the resonance occurs at longer wavelength around λ=350 nm due to its higher refractive index n_a.

When increasing the angle of incidence, these resonances split to two branches resulting in characteristic V-shaped spectra. The reason is that the excitation occurs simultaneously via $+1^{st}$ or -1^{st} diffraction orders at wavelength where the following phase-matching condition is fulfilled:

$$\pm\frac{2\pi}{\lambda}\mathrm{Re}\left\{\sqrt{\frac{n_m^2 n_s^2}{n_m^2+n_s^2}}\right\}=\frac{2\pi}{\lambda}\sin(\theta)+p\frac{2\pi}{\Lambda},$$

where p is the diffraction order and Re{} states for the real part of refractive index. When the angle of incidence is θ=0, the resonance associated with the coupling via p=+1 and -1 overlaps at each interface. However, when the angle of incidence θ deviates from zero, each resonance split to two branches. Figure 4D shows that when the refractive index n_s on the top of the structure is increased by replacing air with water, the short wavelength resonance (SP_s) is red-shifted while the longer wavelength resonance (SP_a) is not changed. The shift of the resonance associated with the excitation of SPs probing the upper interface from λ=214 to 297 nm due to the refractive index change of about δn=0.37 suggests a sensitivity of $S=\delta\lambda/\delta n=224$ nm RIU^{-1}, which is comparable to other diffraction-based SPR sensors [25].

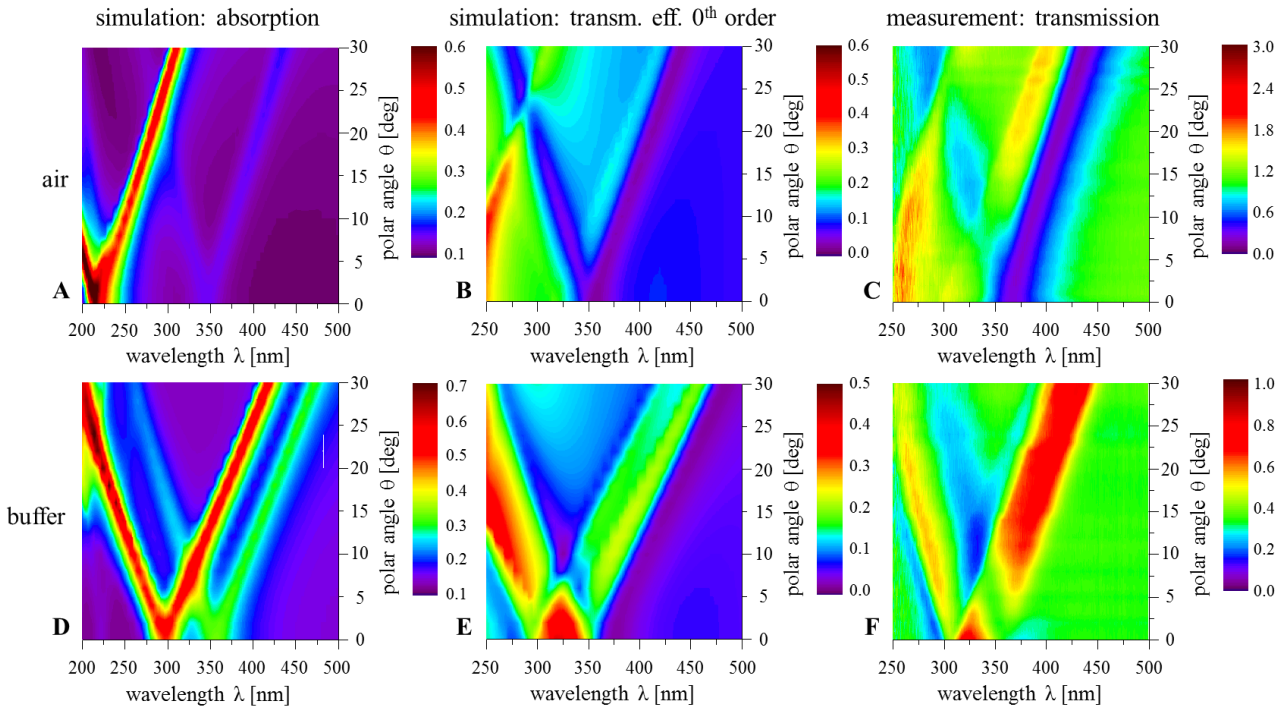

Figure 4. Angle – wavelength dependence of transmission for Al gratings in contact with air (A-C) and TRIS buffer (D-F), respectively. To identify the plasmons, simulations of the absorption are shown for air (A) and buffer (D). Simulations of the expected results of the used grating are shown for air (B) and buffer (E), displaying only the zeroth order, since the higher orders were not collimated into the detector (transm. eff. for transmission efficiency). The measurements are shown for air (C) and buffer (F).

Considering the simulation of the specular transmission (Fig. 4B and E), the resonances occurred at the same wavelengths as the absorption predicts. The resonance coupling to SPs is manifested as peaks or dips due to the interplay of diffraction coupling to SPs and interference of additional out-coupled waves. Except from deviations in the magnitude of intensity, the measured spectra (Fig. 4C: air; Fig. 4F: buffer) are in accordance with the simulations, keeping in mind that minor differences may be attributed to the deviations between the experimentally used and the simulated structure.

The dips of the buffer-metal interface were slightly red-shifted compared to the simulations, the spectral distance between -1st and +1st order resonance wavelength were slightly increased.

UV-SPR probing of protein binding

OBP 14 protein was attached to the grating surface and probed by SPs in the UV range. Fig. 5 shows the acquired transmission spectra for a sample with and without the protein that is compared with simulated absorption for the two polar angles θ=6 and θ=10 deg. These angles were chosen because at θ=6 deg the resonant coupling to SP_s occurred at the main protein absorption band at 280 nm, while at θ=10 deg the resonance is shifted further by 10 nm to the lower wavelength of 270 nm.

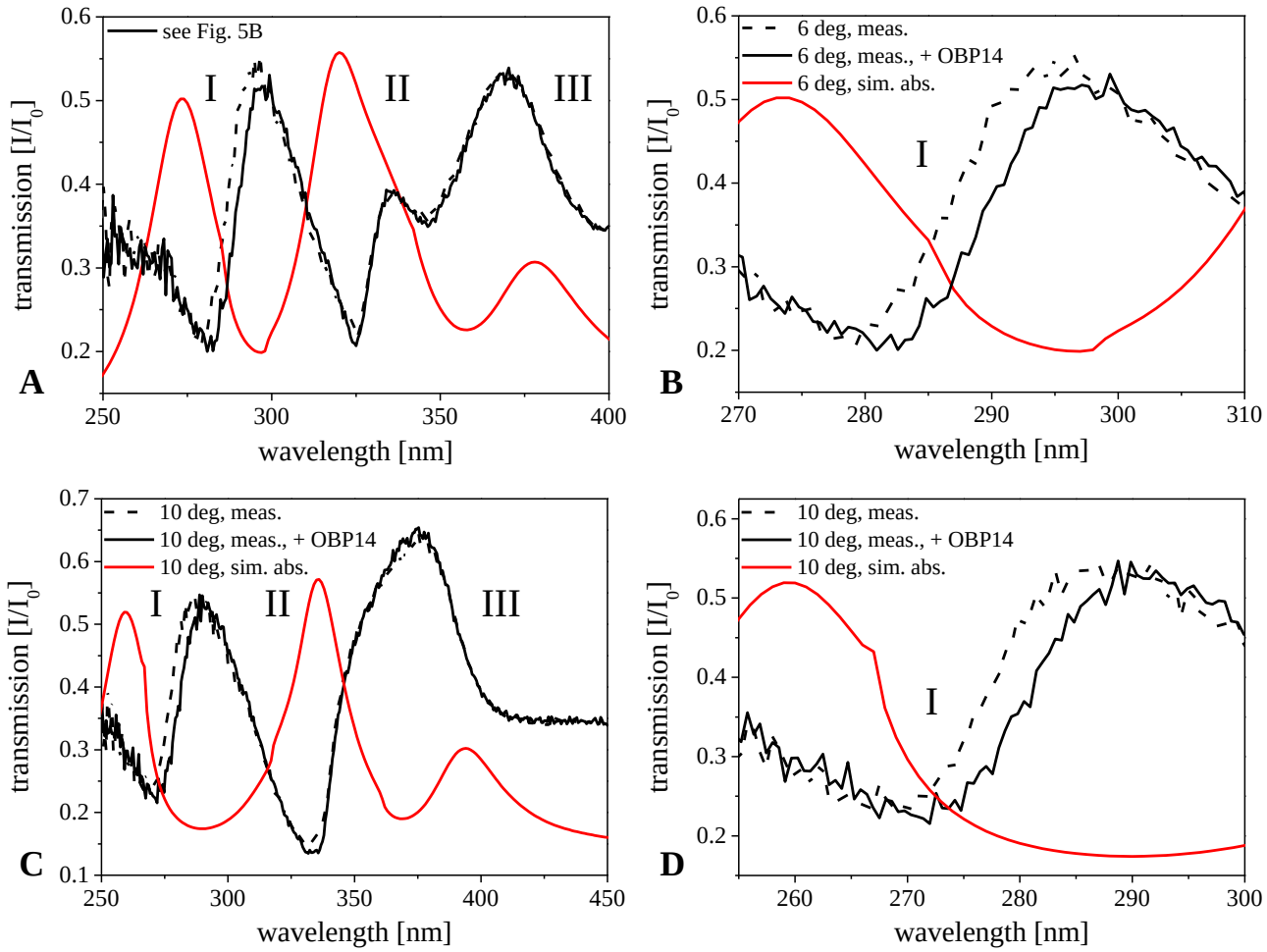

Figure 5. Transmission spectra measured (meas.) before and after protein attachment in comparison to the corresponding simulated absorption (sim. abs.) spectra. (A) θ=6 deg (B) Zoom onto the shift of the resonance wavelength at the metal-buffer interface. (C) θ=10 deg (D) Zoom as in (B) with θ=10 deg.

The transmission dependence on wavelength λ presented in Figure 5 shows three distinct resonance features for the angles θ=6 deg and 10 deg. For θ=6 deg, the dip at λ=280 nm can be assigned to the probing of buffer-metal interface as discussed before (I). The feature at around λ~330 nm can be attributed to the mixed excitation of SP_s and SP_a as the respective dispersions intersected (II). The transmission peak at around λ~370 nm is due to the resonant excitation of SP_a

(III). For the increased angle of incidence to θ=10 deg, the resonance SP_s (I) is blue shifted, the mixed resonance does not shift (II), and the SP_a is red shifted in accordance to the study presented in Figure 4.

After the immobilization of the OBP14 protein (molecular weight of 14 kDa [21]) on the top of the aluminum surface, we can see that only the resonance (I) shifted to a longer wavelength which agrees with the fact that (II) and (III) are associated to the field confinement at the opposite interface. The spectral shift of about ~ 3-4 nm is similar to that measured by diffraction coupled SPR in the red part of spectrum for proteins with similar molecular weight [25]. This observation indicates that OBP protein was immobilized with a density close to a full packed monolayer and that it can be observed in aqueous environment by the developed UV grating coupled SPR sensor.

CONCLUSIONS

We report on the facile implementation of UV-SPR biosensor that is suitable for the *in situ* observation of molecular binding at the aluminum surface. The results clearly indicate the possibility to resonantly excite and interrogate surface plasmons at wavelength of 280 nm. Diffraction coupling to SPR in the UV range exhibit similar sensitivity to that reported on regular gold diffraction grating sensors that operated in the red part of spectrum. The aluminum surface can be functionalized with silane-based linkers for the immobilization of biomolecules with density that is comparable to that observed for regular thiol self-assembled monolayer architectures on gold. The use of the UV wavelength of 280 nm holds potential for the combined measurement of plasmonically amplified auto-fluorescence of proteins. For the developed grating chip, the resonant wavelength can be easily tuned by adjusting the angle of incidence to even lower wavelengths, e.g. towards 260 nm where the DNA exhibits absorption maximum.

ACKNOWLEDGMENT

We thank Prof. Paolo Pelosi and his group at the Department of Biology of Agriculture, Food and Environment, University of Pisa, Italy, for providing the odorant-binding protein 14 of *Apis mellifera* for this and further studies. This was partially supported from the European Union's Horizon 2020 research and innovation program under grant agreement No 633937, project ULTRAPLACAD, under grant agreement No 642787, Marie Sklodowska-Curie Innovative Training Network BIOGEL.

REFERENCES

[1] B. Liedberg, C. Nylander and I. Lundstrom, "Biosensing with Surface-Plasmon Resonance - How It All Started", Biosensors & Bioelectronics, 10(8), R1-R9 (1995).
[2] J. W. Chung, S. D. Kim, R. Bernhardt, et al., "Application of SPR biosensor for medical diagnostics of human hepatitis B virus (hHBV)", Sensors and Actuators B: Chemical, 111–112, 416-422 (2005).
[3] M. Piliarik, L. Párová and J. Homola, "High-throughput SPR sensor for food safety", Biosensors and Bioelectronics, 24(5), 1399-1404 (2009).
[4] G. Naik, J. Kim, N. Kinsey, et al., "Alternative Plasmonic Materials", Modern Plasmonics, 4, 189-221 (2014).
[5] M. W. Knight, N. S. King, L. F. Liu, et al., "Aluminum for Plasmonics", ACS Nano, 8(1), 834-840 (2014).
[6] D. Gerard and S. K. Gray, "Aluminium plasmonics", Journal of Physics D: Applied Physics, 48(18), (2015).
[7] S. Babar and J. H. Weaver, "Optical constants of Cu, Ag, and Au revisited", Applied Optics, 54(3), 477-481 (2015).
[8] K. M. McPeak, S. V. Jayanti, S. J. P. Kress, et al., "Plasmonic Films Can Easily Be Better: Rules and Recipes", ACS Photonics, 2(3), 326-333 (2015).
[9] R. P. H. Kooyman, "Physics of Surface Plasmon Resonance", Handbook of Surface Plasmon Resonance, 15-34 (2008).
[10] A. Ono, M. Kikawada, R. Akimoto, et al., "Fluorescence enhancement with deep-ultraviolet surface plasmon excitation", Optics Express, 21(15), 17447-17453 (2013).
[11] K. Ray, M. H. Chowdhury and J. R. Lakowicz, "Aluminum nanostructured films as substrates for enhanced fluorescence in the ultraviolet-blue spectral region", Analytical Chemistry, 79(17), 6480-6487 (2007).

[12] M. Lee, J. U. Kim, K. J. Lee, et al., "Aluminum Nanoarrays for Plasmon-Enhanced Light Harvesting", ACS Nano, 9(6), 6206-6213 (2015).
[13] J. Olson, A. Manjavacas, L. F. Liu, et al., "Vivid, full-color aluminum plasmonic pixels", Proceedings of the National Academy of Sciences of the United States of America, 111(40), 14348-14353 (2014).
[14] Y. Ekinci, H. H. Solak and J. F. Loffler, "Plasmon resonances of aluminum nanoparticles and nanorods", Journal of Applied Physics, 104(8), (2008).
[15] C. Langhammer, M. Schwind, B. Kasemo, et al., "Localized surface plasmon resonances in aluminum nanodisks", Nano Letters, 8(5), 1461-1471 (2008).
[16] C. Forestiere, A. Handin and L. Dal Negro, "Enhancement of Molecular Fluorescence in the UV Spectral Range Using Aluminum Nanoantennas", Plasmonics, 9(3), 715-725 (2014).
[17] S. Katti, N. Lokhande, D. Gonzalez, et al., "Quantitative analysis of pheromone-binding protein specificity", Insect Molecular Biology, 22(1), 31-40 (2013).
[18] R. Mastrogiacomo, I. Iovinella and E. Napolitano, "New fluorescent probes for ligand-binding assays of odorant-binding proteins", Biochemical and Biophysical Research Communications, 446(1), 137-142 (2014).
[19] G. N. Wogan, "Chemical Nature and Biological Effects of the Aflatoxins", Bacteriological Reviews, 30(2), 460-470 (1966).
[20] I. H. Malitson, "Interspecimen Comparison of the Refractive Index of Fused Silica", Journal of the Optical Society of America, 55(10), 1205-1209 (1965).
[21] S. Spinelli, A. Lagarde, I. Iovinella, et al., "Crystal structure of Apis mellifera OBP14, a C-minus odorant-binding protein, and its complexes with odorant molecules", Insect Biochemistry and Molecular Biology, 42(1), 41-50 (2012).
[22] E. D. Palik, "Handbook of Optical Constants of Solids", 3 (1998).
[23] G. M. Hale and M. R. Querry, "Optical Constants of Water in the 200-nm to 200-μm Wavelength Region", Applied Optics, 12(3), 555-563 (1973).
[24] P. E. Ciddor, "Refractive index of air: new equations for the visible and near infrared", Applied Optics, 35(9), 1566-1573 (1996).
[25] P. Adam, J. Dostálek and J. Homola, "Multiple surface plasmon spectroscopy for study of biomolecular systems", Sensors and Actuators B: Chemical, 113(2), 774-781 (2006).